Lasers in Eng., Vol. 46, pp. 383–393
Reprints available directly from the publisher
Photocopying permitted by license only

Debris-free, Zero Taper Cutting of BOROFLOAT 33 Glass Using a Femtosecond Bessel Laser Beam

Z-Q. LI[1], J-L. WANG[2], X-F. WANG[2], O. ALLEGRE[1], W. GUO[1], W-Y. GAO[2], Y. XUE[2] AND LIN LI[1,*]

[1]*Laser Processing Research Centre, Department of Mechanical, Aerospace and Civil Engineering, The University of Manchester, Oxford Road, Manchester, M13 9PL, UK*
[2]*Beijing Institute of Aerospace Control Devices, 52 Yongdong Road, Beijing 100039, China*

Owing to nonlinear absorption, ultra-short pulse lasers can be used to modify the properties of bulk transparent materials. In this paper, an 800 nm femtosecond laser Bessel beam was used to induce nonlinear filamentation inside a bulk BOROFLOAT 33 borosilicate glass sheet, followed by mechanical cleavage. The effects of scanning speed on the cleavage force and surface roughness were analysed. By increasing the number of lasers passes over the test piece, the cleavage force was reduced while the sidewall surface roughness was increased. By optimizing the process parameters, straight and curved cuts have been achieved free from debris and crack, with a zero taper a surface roughness around 550 nm Ra.

Keywords: Ti:Sapphire femtosecond laser, BOROFLOAT 33 glass, surface roughness, Bessel beam, filament, scanning passes, bending force

1 INTRODUCTION

BOROFLOAT 33 borosilicate glass is widely used in the consumer electronics industry for example to produce micro-electro-mechanical systems (MEMS), flat displays or cover glass packaging Cutting this type of glass presents a number of challenges, such as achieving zero taper, zero cut width, debris-free and ultra-smooth surface roughness. The traditional method for glass cutting is dominated by diamond tool-based scoring and break cutting

*Corresponding author: E-mail: lin.li@manchester.ac.uk

[1]; however, this is limited by poor surface finish with microcracks, which often leads to reduced product life. To increase the products quality, extra grinding and polishing steps are normally required as post processing. Advanced cutting methods such as hot air jet cutting [2], or water jet cutting [3], have been developed and used for decades. But all these methods have drawbacks [4]. Laser-based glass cutting [5] offers an attractive alternative propagation [6], laser melting and evaporation [7], and short pulse laser ablation [8]. Laser scribing and breaking typically induces defects to the cut surface, and post processing is normally required. For controlled fracture propagation, an initial crack is necessary. The laser melting and evaporation method typically produces poor edge quality so post processing is necessary, whereas the short pulse laser ablation method often leads to cracks and debris.

Due to the nonlinear absorption effect of the ultra-short pulsed laser beam, materials can be processed even though the material is transparent at the laser wavelength [9]. The method to cut transparent materials through the highly localized material property modification called stealth dicing. Based on the beam focusing situation inside of the material, stealth dicing can be divided into the generation of dotted lines [10], elongated spots [11] and laser filamentation [12].

In this paper the focusing of non-diffractive Bessel beam [13-15] was selected as it generates almost invariant nonlinear propagation inside of the transparent material [16]. The effects of process parameters such as scanning speed and scanning passes on the quality of BOROFLOAT 33 glass Bessel beam cutting have been analysed. Straight and curved cuts of high quality BOROFLOAT 33 glass have been achieved, with a zero taper, no debris or cracks, and a sidewall surface roughness smaller than 550 nm Ra.

2 EXPERIMENTAL METHODS

A Ti:Sapphire femtosecond laser (Libra Ti:Sapphire; Coherent, Inc.) was used at an 800 nm wavelength with a 100 femtosecond pulse duration, a 1 kHz repetition rate, M^2 smaller than 1.5, an output power of up to 1 W, with an approximately Gaussian beam intensity distribution and a raw beam diameter of 5 mm. Neutral density filters and a polarization attenuator were applied to controlling the pulse energy. A quarter waveplate (WPQ10ME-780; Thorlabs, Inc.) and a s-waveplate (RPC-800-08; Altechna) were applied to transforming linear polarization to circular polarization or radial/azimuthal polarization. A beam reducer was placed into the beam path to reduce the diameter of the Gaussian beam from 5 mm into 1.25 mm. A 20^o physical angle axicon lens was used to focus the Gaussian beam into a non-diffractive Bessel beam. BOROFLOAT 33 glass with thickness of 0.5, 1.0 and 1.5 mm were placed on a three-axis translation computer numerical control (CNC) stage. A schematic of the experimental arrangement is shown in Figure 1.

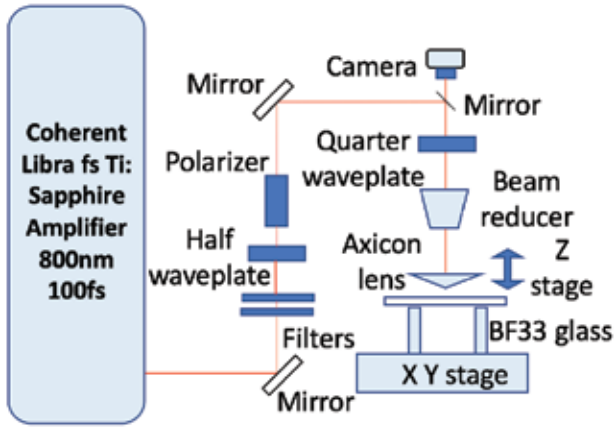

FIGURE 1
Schematic representation of the experimental arrangement.

To realise BOROFLOAT 33 glass cutting the test pieces were placed in the central area of the non-diffractive Bessel beam. Filament was generated inside the BOROFLOAT 33 glass from its top surface and reaching its bottom surface. After laser processing a mechanical force was applied to separate the cuts. Figure 2 shows the example circular contours generated with the induced filaments by using an optical microscope (VHX 5000; Keyence Corporation). For standard cleavage, straight line contour is normally preferred.

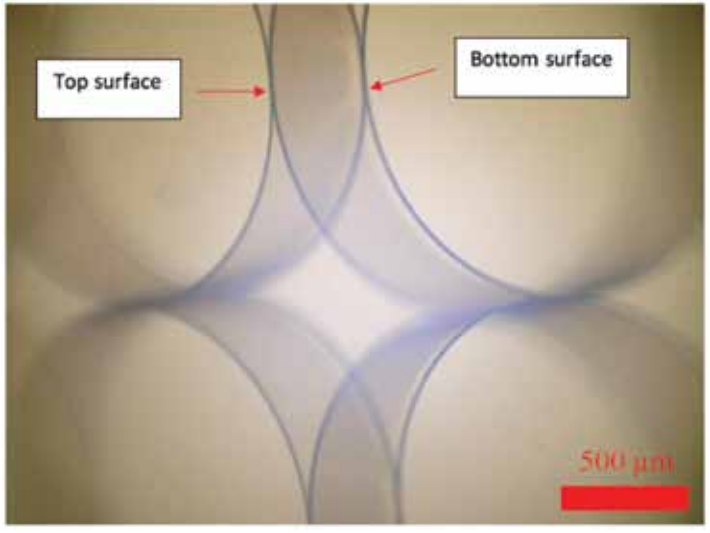

FIGURE 2
Optical micrograph showing the filaments generated inside of BOROFLOAT 33 glass.

Based on the following [17] the central core diameter and the central core length of the Bessel beam can be calculated and are found to be 1.8 μm and 3.6 mm, respectively:

$$n \sin \alpha = \sin(\alpha + \beta) \tag{1}$$

$$r = \frac{1.2024\lambda}{\pi \sin \beta} \tag{2}$$

and

$$L = \frac{\omega_0}{2 \tan \beta} \tag{3}$$

where n is the refractive index of the fused silica, α is the physical angle of the axicon lens, β refers to the deflection angle of the Bessel beam, λ refers to the wavelength of laser beam and ω_o is the illuminated beam diameter. After the cutting process the sidewall quality was analysed with a white light interferometer (Contour GT-K; Veeco Instruments, Inc.) and an optical microscope (DM/LM; Leica Microsystems, GmbH).

3 RESULTS AND DISCUSSION

3.1 Bessel beam filamentation

A microscopic study of the inscribed contours was used to optimise the pulse overlap prior to the subsequent cutting experiments. Figure 3 shows the microstructures produced with 450 μJ pulse energy with increasing scanning speeds from 1 to 7 mm/s, where the beam pulses were gradually separated from each other. In a high overlap situation it can be seen that the BOROFLOAT 33 glass incurred significant thermal damage. Large amounts of debris was induced and attached around the processing area, as can be seen from Figure 3(a). As expected, increasing the scanning speed led to a decrease of pulse overlap. It can be noticed that only the central core of the Bessel beam interacted with the material. It means that the intensity of the high order rings of the Bessel beam was below the optical breakdown threshold. Additionally, the diameter of the central core can be measured to be around 2.3 μm, which is larger than the theoretical value of 1.8 μm given above. It means the applied pulse energy largely exceeded the threshold intensity.

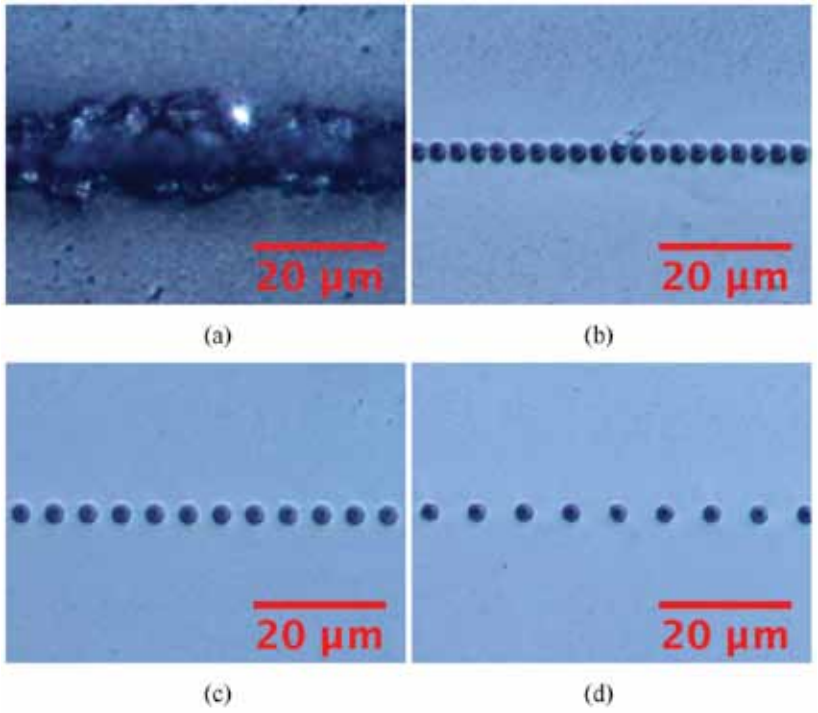

FIGURE 3
Optical micrographs showing the top view of the Bessel beam pulses separation with scanning speed of (a) 1 mm/s, (b) 3 mm/s, (c) 5 mm/s and (d) 7 mm/s.

3.2 Effects of scanning speed on cutting quality

To analyse the BOROFLOAT 33 glass cleavage parameters the glass sheets with different thicknesses were cut into 10×50 mm^2 squares. By performing Bessel beam processing in the central area of the material, filaments were induced; subsequently, the processed material was cleaved by using a three-point bending micro-test device (5 kN Tensile Tester; DEBEN UK, Ltd.). The effects of scanning speed on the bending force for the different thicknesses of BOROFLOAT 33 glass are shown in Figure 4.

It can be seen from Figure 4 that for the 0.5 mm thickness glass the scanning speed did not affect the bending force in any significant way, albeit with a low point around 4 mm/s. The BOROFLOAT 33 glass plates with thicknesses of 1.0 and 1.5 mm also featured a low point roughly in the same scan speed region - 3 mm/s in the case of the 1.0 mm thick workpiece. Low scan speeds below that point did not induce a strong correlation with bending force; however, above 4 mm/s there was a clear linear relationship between scan speed and bending force for these thicknesses.

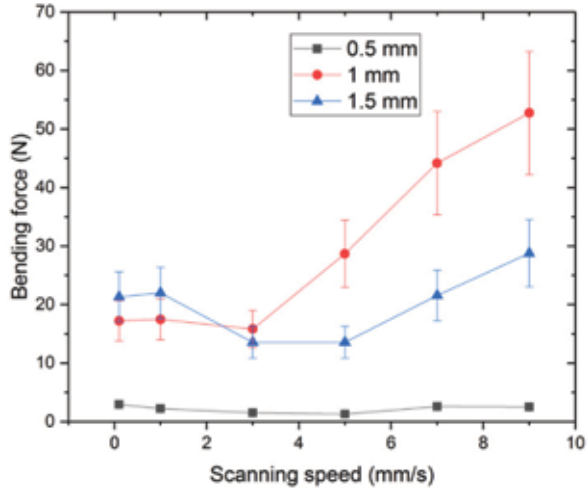

FIGURE 4
Graph showing the required bending force *versus* scan speed for cutting BOROFLOAT 33 glass sheet samples with 450 μJ pulse energy.

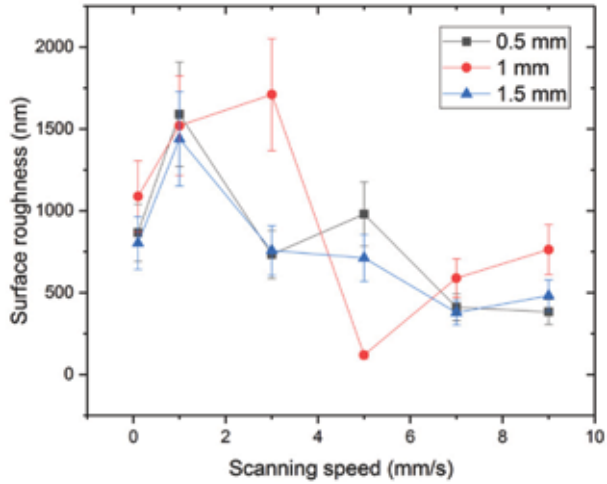

FIGURE 5
Graph showing the sidewall surface roughness *versus* scan speed for cutting BOROFLOAT 33 glass sheet samples with 450 μJ pulse energy.

The effects of scanning speed on the sidewall surface roughness were investigated. Figure 5 shows that the surface roughness varied significantly within the selected range of scan speeds. Peaks of high surface

roughness above 1500 nm Ra were seen at fairly low scan speed values of 1 mm/s for the 0.5 and 1.5 mm thick plates, and 3 mm/s for the 1.0 mm thick plate. The surface roughness showed a decreasing trend with increasing scan speed for the 0.5 and 1.5 mm thick plates, although the 1.0 mm tick plate did not produce a clear trend. For lower scanning speeds of 0.1 mm/s, lower surface roughness for 0.5, 1.0 and 1.5 mm thick plates were achieved, which was due to the high pulse overlap, but the efficiency was reduced

For all subsequent cutting experiments, a cutting scan speed of 4 mm/s was chosen, since it represented an optimum value where the bending force and surface roughness were low for most plate thicknesses.

3.3 Effects of scanning passes on cutting quality

The effects of the number of scanning passes on the cutting quality was investigated next. A 450 μJ pulse energy laser beam with a 4 mm/s scanning speed was used and the number of scanning passes was increased from 1 to 15 passes on the 1.0 mm thickness BOROFLOAT 33 glass. Under this scanning speed the laser pulses were separated. During the over scan, laser pulses may not interact with the same region but did interact with the same scanning line, weakening the material along the line. The trends of bending force and sidewall surface roughness are shown in Figure 6 and Figure 7, respectively.

In Figure 6 a clear trend can be seen where the required bending force was gradually reduces as the scanning passes increased until around 12

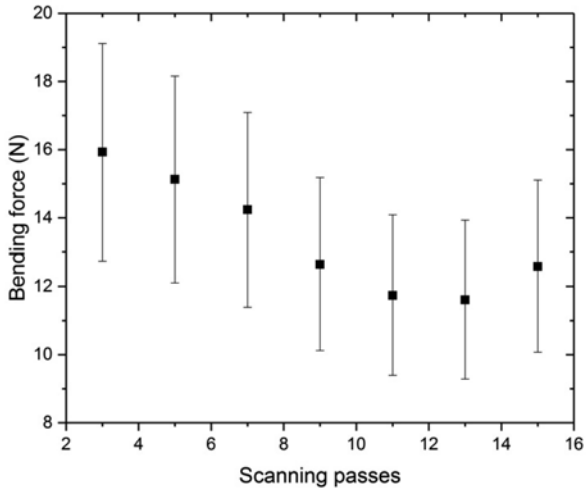

FIGURE 6
Graph showing the required bending force *versus* number of scans passes for cutting BOROFLOAT 33 glass sheet samples with 450 μJ pulse energy.

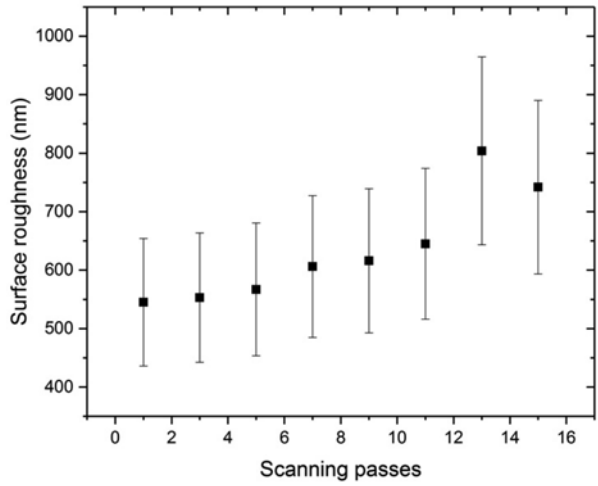

FIGURE 7
Graph showing the sidewall surface roughness *versus* number of scans passes for cutting BOROFLOAT 33 glass sheet samples with 450 μJ pulse energy.

passes. For more scanning passes, the bending force was not reduced again, and there was even some increase. In Figure 7 it can be seen that the sidewall surface roughness gradually increased with increasing scanning passes number. This highlights a trade-off between bending force and surface roughness in glass cutting, where an increase in the scanning passes leads to easier cleaving (i.e. lower bending force), however this is at the expense of higher surface roughness.

3.4 BOROFLOAT 33 glass cutting

Having identified suitable processing windows for cutting the thicknesses of BOROFLOAT 33 glass sheet available, various geometries and size were cut using straight and curved contours representative of applications found in the consumer electronic industry. Figure 8 shows example geometries created by using 450 μJ pulse energy, 4 mm/s scanning speed single pass. It can be seen that the cutting quality was high with no crack or debris. In all cases, the side wall surface roughness was at or less than 550 nm Ra.

4 CONCLUSIONS

An 800 nm Bessel Ti:Sapphire femtosecond laser beam was used to generate filamentation inside of BOROFLOAT 33 borosilicate glass, followed by mechanical cleavage. The effects of the scanning speed on the quality (cleav-

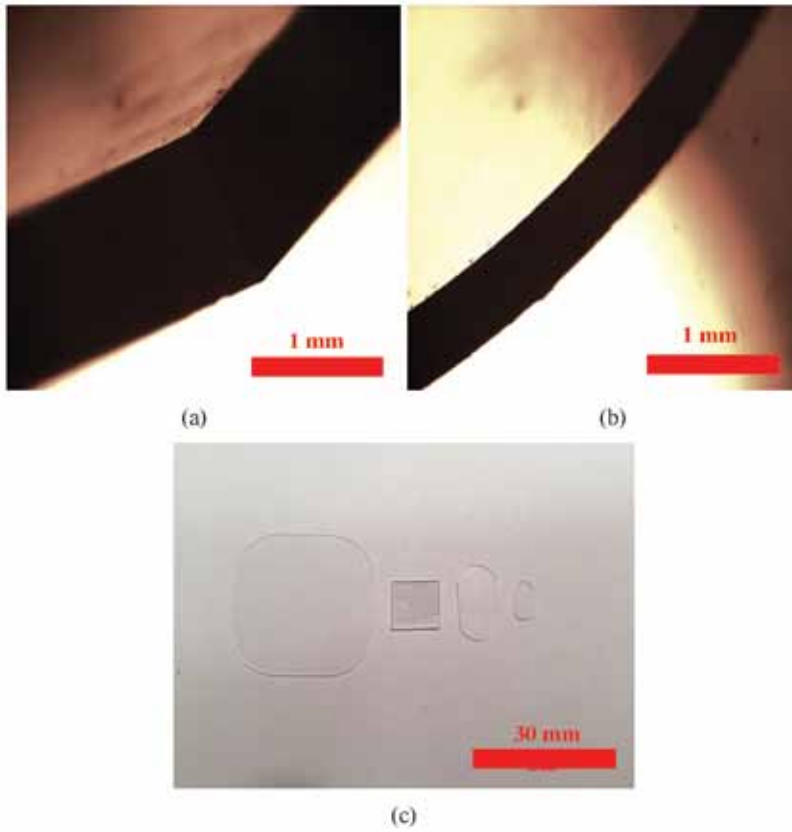

FIGURE 8
Optical micrographs showing BOROFLOAT 33 glass sheet cut with 450 μJ pulse energy. (a) Magnified view showing cuts along a curved contour of 5 mm radius, (b) magnified view showing cuts along a curved contour 10 mm radius and (c) overall views showing various geometries and thicknesses.

age force and sidewall surface roughness) of BOROFLOAT 33 glass Bessel beam cutting have been discussed. With the increase of number of scanning passes, the required cleavage force can be reduced, although the sidewall surface roughness was increased to some extent. Straight and curved cuts have been achieved free from debris and crack, with zero taper a surface roughness around 550 nm Ra or less.

ACKNOWLEDGMENT

This research was partially supported by the National Key R&D Program of China (2017YFB1104604).

NOMENCLATURE

L	Central core length of the Bessel beam (m)
n	Refractive index of the fused silica
r	Central core diameter of the Bessel beam (m)

Greek symbols

α	Physical angle of the axicon lens (^{o})
β	Deflection angle of the Bessel beam (^{o})
λ	Wavelength of the laser beam (m)
ω_o	Illumited beam diameter (m)

REFERENCES

[1] Zhou M., Ngoi B.K.A., Yusoff M.N. and Wang X.J. Tool wear and surface finish in diamond cutting of optical glass. *Journal of Materials Processing Technology* **174**(1-3) (2006), 29–33.

[2] Prakash E.S., Sadashivappa K., Joseph V. and Singaperumal M. Nonconventional cutting of plate glass using hot air jet: Experimental studies. *Mechatronics* **11**(6) (2001), 595–615.

[3] Yuan F., Allred D.D., Johnson J.A. and Todd R.H. Waterjet cutting of cross-linked glass. *Journal of Vacuum Science and Technology A: Vacuum, Surfaces and Films* **13**(1) (1995), 136–139.

[4] Nisar S., Li L. and Sheikh M.A. Laser glass cutting techniques - A review. *Journal of Laser Applications* **25**(4) (2013), 042010.

[5] Ishikawa T., Ueda T., Furumoto T., Hosokawa A. and Tanaka R. Thermal stress cleaving of brittle materials by laser beam. *CIRP Annals* **51**(1) (2002), 149-152.

[6] Xu J., Hu H., Zhuang C., Ma G., Han J. and Lei Y. Controllable laser thermal cleavage of sapphire wafers. *Optics and Lasers in Engineering* **102** (2018), 26–33.

[7] Wang Z.K., Zheng H.Y., Seow W.L. and Wang X.C. Investigation on material removal efficiency in debris-free laser ablation of brittle substrates. *Journal of Materials Processing Technology* **219** (2015), 133–142.

[8] Strigin M.B. and Chudinov A.N. Cutting of glass by picosecond laser radiation. *Optics Communications* **106**(4-6) (1994), 223–226.

[9] Savriama G., Semmar N., Barreau L. and Boulmer-Leborgne C. Experimental and numerical analysis of crack-free DPSS laser dicing of borosilicate glass. *Applied Physics A: Materials Science & Processing* **119**(2) (2015), 559–569.

[10] Ahmed F., Lee M.S., Sekita H., Sumiyoshi T. and Kamata M. Display glass cutting by femtosecond laser induced single shot periodic void array. *Applied Physics A: Materials Science & Processing* **93**(1) (2008),189–192.

[11] Bovatsek J.M., Arai A.Y. and Yoshino F. *Transparent Material Processing with an Ultrashort Pulse Laser*. US Patent US 20070051706 A1, 8th March 2007.

[12] Abbas H.S. and Herman P.R. *Method of Material Processing by Laser Filamentation*. US Patent US 10399184 B2, 28th March 2016.

[13] Duocastella M. and Arnold C.B. Bessel and annular beams for materials processing. *Laser & Photonics Reviews* **6**(5) (2012), 607-621.

[14] McGloin D. and Dholakia K. Bessel beams: Diffraction in a new light. *Contemporary Physics* **46**(1) (2005), 15–28.

[15] Meyer R., Giust R., Jacquot M., Dudley J.M. and Courvoisier F. Submicron-quality cleaving of glass with elliptical ultrafast Bessel beams. *Applied Physics Letters* **111**(23) (2017), 231108.

[16] Courvoisier F., Zhang J., Bhuyan M.K. Jacquot M. and Dudley J.M. Applications of femtosecond Bessel beams to laser ablation. *Applied Physics A: Materials Science & Processing* **112**(1) (2013), 29–34.

[17] Dudutis J., Gečys P. and Račiukaitis G. Non-ideal axicon-generated Bessel beam application for intra-volume glass modification. *Optics Express* **24**(25) (2016), 28433.